Nonlinear Dyn (2016) 85:97–106
DOI 10.1007/s11071-016-2670-z

ORIGINAL PAPER

Control parameter design for automatic carrier landing system via pigeon-inspired optimization

Yimin Deng · Haibin Duan

Received: 13 September 2015 / Accepted: 3 February 2016 / Published online: 12 March 2016

Abstract In this paper, a novel control parameter design method is presented for the automatic carrier landing system. To overcome difficulties in the manual parameter adjustment task, the pigeon-inspired optimization algorithm is utilized by converting the parameter design problem to an optimization problem. The modified version is proposed to avoid the lack of the diversity of pigeon population in the basic version. Parameters in the inner loop are optimized by computing the fitting difference between an ideal frequency response curve and the frequency response curve of the optimized control system. To optimize control parameters in the H-dot autopilot and the approach power compensation system, a weighted linear cost function in the time domain is adopted. Series of experiments are conducted to demonstrate the feasibility and effectiveness of our method. Comparative results indicate that out method is much better than other methods.

Keywords Automatic carrier landing system · Control parameter design · Pigeon-inspired optimization

Y. Deng · H. Duan (✉)
State Key Laboratory of Virtual Reality Technology and Systems, School of Automation Science and Electrical Engineering, Beihang University (BUAA), Beijing 100191, People's Republic of China
e-mail: hbduan@buaa.edu.cn

1 Introduction

Landing an aircraft on a carrier is a demanding task. As unwanted ship motions and the air turbulence exist, achieving the narrow landing window requires precision control of the flight path [1]. To help relieve the pilot and perform tightly coordinated control of aircraft motions and airspeed, the automatic carrier landing system (ACLS) has been developed. In general, the ACLS incorporates a shipboard tracking radar, a radio data link, the control system and the digital computer [2]. It can provide the automatic control of the flight path and approach velocity. After measuring the aircraft's position using the tracking radar, the corrective control commands are calculated and transmitted to the aircraft to generate the precision flight path.

In the control system, the H-dot control command has been devised and widely used to keep the touchdown error small [3]. The H-dot control command is observed and followed to ensure the aircraft track the glide slope accurately. On the basis of the H-dot control law, the ACLS commonly incorporates the inner loop control system, the approach power compensation system (APCS) and the H-dot command autopilot. The inner loop control system is employed to increase the handing quality, while the APCS is utilized to maintain a constant angle of attack when the aircraft is landing [4,5]. The H-dot autopilot is designed to follow the H-dot control command, which has been proved to be effective in alleviating the influence of air turbulence [6,7].

To design the controller for the ACLS, different approaches have been investigated, such as the traditional PID controller [2], the F/A-18 fuzzy logic controller [8], finite horizon H-infinity techniques [9], the robust controller [10] and so on [11–14]. To achieve the satisfied performance, parameters in the control system have to be adjusted with experience. Adjusting parameters is a difficult and time-consuming task, especially when the control system has the coupled control structure with a large number of parameters.

To overcome the control parameter design problem, optimization tools have been considered [15–20]. The parameter design problem can be converted to an optimization problem, which can be easily solved through the fitness function. The pigeon-inspired optimization (PIO) algorithm is a newly proposed swarm intelligence method, which mimics the homing behavior of pigeons [21]. The PIO algorithm has been proved to possess a better performance compared with other algorithms like genetic algorithm (GA) and particle swarm optimization (PSO) algorithm [22–25]. In this paper, a modified version is presented by introducing a probability factor for the operator selection. Then, the algorithm is applied to optimize control parameters in the inner loop and the H-dot autopilot with the APCS, respectively. The fitness function of the inner loop optimization is designed by computing the fitting difference between the frequency response curve of the optimized control system and an ideal frequency response curve. A weighted linear cost function in the time domain is adopted for the control parameter optimization in the H-dot autopilot and the APCS. The contribution of the paper is described as follows: (1) the control parameter design task is converted to an optimization problem, and the PIO algorithm is introduced to automatically optimizing the control parameters in the automatic carrier landing system; (2) the modified PIO (MPIO) algorithm is proposed by introducing a probability factor for the operator selection and implementing the local gather strategy for all pigeons not only for the decreased number of pigeons.

This paper is structured as follows: Sect. 2 introduces the control structure of the automatic carrier landing system. To convert the control parameter design problem to the optimization problem, the cost functions are expatiated in this section. In Sect. 3, the basic PIO algorithm and its modified version are presented. Comparative experiments are conducted in Sect. 4. Our concluding remarks are given in the final section.

2 Preliminary

2.1 Control structure of the automatic carrier landing system

The longitudinal small turbulence dynamic model of F/A-18A is given by [20]

$$\begin{cases} \dot{x} = Ax + Bu \\ y = Cx + Du \end{cases} \tag{1}$$

In Eq. (1), $x = (\Delta u/V_0, \Delta\alpha, \Delta\theta, \Delta q, \Delta h/V_0)^T$, $y = (\Delta h, \Delta\gamma, \Delta n_z/V_0, \Delta\alpha, \Delta u, \Delta\theta, \Delta q)^T$, and $u = (\Delta\delta_s, \Delta\delta_{LEF}, \Delta\delta_{PL})^T$, where Δu, $\Delta\alpha$, $\Delta\theta$, Δq, $\Delta\gamma$, Δn_z, Δh are the turbulence of velocity, angle of attack, angle of pitch, pitch rate, flight path angle, normal accelerate and height, respectively. $\Delta\delta_s$ is the deflection of stabilator, $\Delta\delta_{LEF}$ is the deflection of leading-edge flap and $\Delta\delta_{PL}$ is the output of throttle. Based on plant matrices of the F/A-18A longitudinal system in [9], the system matrices A, B, C and D in this paper are listed in Table 1.

Table 1 Matrices of the F/A-18A longitudinal system

$$A = \begin{bmatrix} -0.0705 & 0.0475 & -0.1403 & 0.0000 & -0.000058 \\ -0.3110 & -0.3430 & 0.0000 & 0.99133 & 0.00102 \\ 0.0000 & 0.0000 & 0.0000 & 1.0000 & 0.0000 \\ 0.0218 & -1.1660 & 0.0000 & -0.2544 & 0.0000 \\ 0.0000 & -1.0000 & 1.0000 & 0.0000 & 0.0000 \end{bmatrix}$$

$$B = \begin{bmatrix} 0.0121 & 0.00248 & 0.2316 & 0.0475 \\ -0.0721 & 0.0140 & -0.0338 & -0.3430 \\ 0.0000 & 0.0000 & 0.0000 & 0.0000 \\ -1.8150 & -0.0790 & 0.0023 & -1.1660 \\ 0.0000 & 0.0000 & 0.0000 & 1.0000 \end{bmatrix}$$

$$C = \begin{bmatrix} 0 & 0 & 0 & 0 & 69.96 \\ 0 & -1 & 1 & 0 & 0 \\ 0.311 & 0.343 & 0 & 0.0087 & -0.001 \\ 0 & 1 & 0 & 0 & 0 \\ 69.96 & 0 & 0 & 0 & 0 \\ 0 & 0 & 1 & 0 & 0 \\ 0 & 0 & 0 & 1 & 0 \end{bmatrix}$$

$$D = \begin{bmatrix} 0 & 0 & 0 & 0 \\ 0 & 0 & 0 & 0 \\ 0.0721 & -0.0140 & 0.0338 & 0.3430 \\ 0 & 0 & 0 & 1 \\ 0 & 0 & 0 & 0 \\ 0 & 0 & 0 & 0 \\ 0 & 0 & 0 & 0 \end{bmatrix}$$

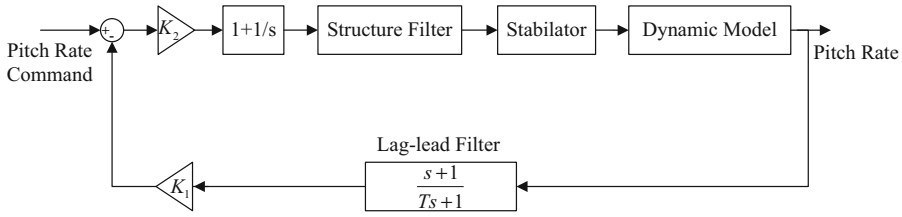

Fig. 1 Inner loop in ACLS

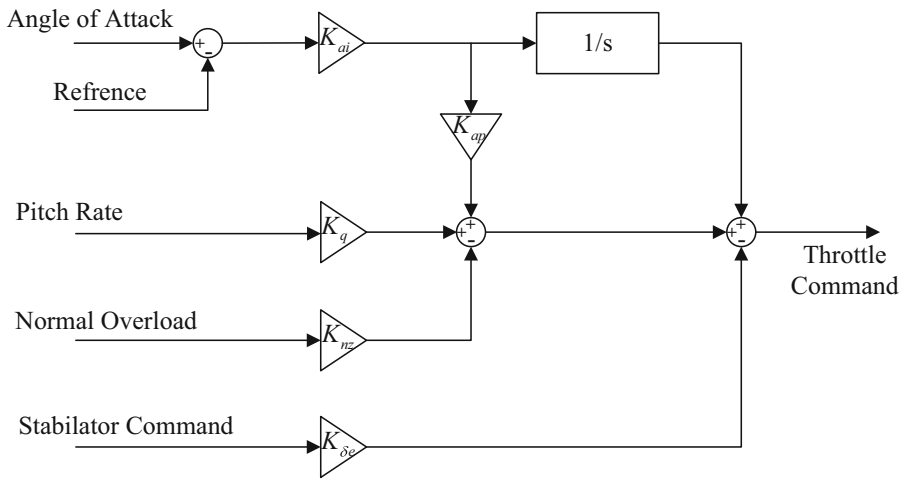

Fig. 2 Structure of the APCS

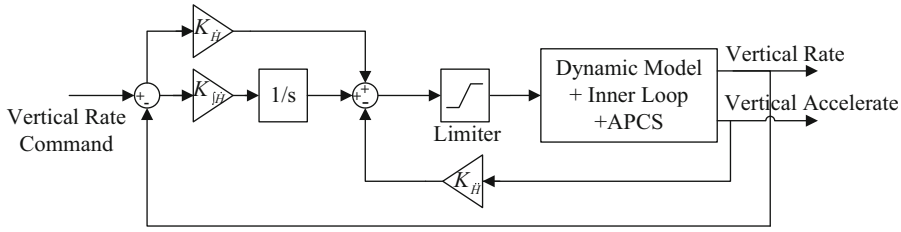

Fig. 3 Structure of the H-dot autopilot in APCS

On the basis of the aircraft model, the ACLS is designed to be composed of three parts: the inner loop, the APCS and the H-dot autopilot. In fact, the controller for the ACLS in this paper is similar to the traditional PID controller, which is simpler than other controllers such as the fuzzy logic controller [8] and the H-infinity controller [9,26]. In the control structure of the inner loop as shown in Fig. 1, the pitch rate is controlled to achieve rapid dynamic response. A structure filter and a lag-lead filter are utilized in the feedback loop. The parameter T in the lag-lead filter is able to affect the amplitude–frequency curve of the inner loop. Two parameters are introduced as the gain values in the forward and feedback path, respectively. Therefore, the dynamic response to the vertical rate command can be obtained through adjusting these three parameters.

The low-order approximations for the actuator and structure filter models are given as:

$$\text{Stabilator: } \frac{\delta_H}{\delta_{H_{cm}}} = \frac{1325}{s^2 + 29.85s + 1325} \tag{2}$$

$$\text{Structure filter: } F(s) = \frac{s^2 + 3.6s + 3600}{s^2 + 87s + 4270} \tag{3}$$

To ensure the aircraft trace a landing path with the constant angle of attack and velocity, the APCS is applied to obtain the throttle command. As shown in Fig. 2, four signals are introduced in the APCS as the feedback signals. The angle of attack is designed to trace a constant. The pitch rate signal can increase the damping ratio. The stabilator command signal can relieve the deflection of the stabilator. In addition, the vertical rate of the landing aircraft is controlled by the H-dot command autopilot as shown in Fig. 3. In general, the vertical rate can be described as $\dot{H} = V \sin\gamma$, where V is the velocity and γ is the flight path angle. To maintain the aircraft trace a landing path, the con-

trol of the path angle can be converted to the control of the vertical rate. Thus, the H-dot command autopilot utilizes the vertical rate signal as the feedback signal. To guarantee the capability of the system, the pitch rate command limiter is employed to ensure the pitch rate command within the limit of 3 deg/s. To increase the damping ratio, the vertical accelerate signal is introduced in the feedback loop.

2.2 Problem formulation

Subject to the dynamic model and the control structure, the purpose of optimization is to find proper parameters which are capable of ensuring the aircraft trace a landing path precisely. In real applications, it is a tedious and time-consuming work to adjust control parameters manually. What's more, the best control performance usually cannot be achieved through empirical tests under given constraints and configurations. There is a need to automatically obtain control parameters. Using optimization tools, the control parameter design problem can be converted to an optimization problem, and thus, optimal parameters can be obtained.

In this paper, a modified pigeon-inspired optimization (MPIO) algorithm is presented to design parameters in the control structure of ACLS. The inner loop and autopilot loop are optimized, respectively. Cost functions of the inner loop and ACLS are designed in this section. Three parameters in the inner loop are obtained through fitting two frequency response curves. After fixing the inner loop, eight parameters in the H-dot autopilot and APCS are optimized by ensuring the aircraft follow the predefined vertical rate command.

2.3 Inner loop control parameter optimization

Given the control structure of the inner loop as shown in Fig. 1, parameters are optimized by comparing the frequency response curve with a reference curve. Three control parameters are optimized in the inner loop. Thus, the dimension of the inner loop control parameter optimization problem is three. The solution can be represented as a 3-D vector $X_i = [K_1, K_2, T]$. The actual frequency response curve of the F/A-18A inner loop is adopted as the reference one. To ensure requirements of the control system, the frequency response curve should approach to the reference one. Therefore, the cost function is designed based on the error of fitting. The cost function is defined as [20]

$$f = \sum_{i=1}^{N_S} (G - G_R)^2 \tag{4}$$

where N_S is the number of sampling points, G is the amplitude-frequency curve of the inner loop and G_R is the reference curve.

2.4 ACLS control parameter optimization

As shown in Figs. 2 and 3, control parameters in two components (i.e., the APCS and the H-dot autopilot loop) should be obtained. As two components couple with each other, control parameters are optimized simultaneously. Therefore, the solution is defined as a vector including eight parameters:

$$X_i = [K_{ai}, K_{ap}, K_{nz}, K_q, K_{\delta e}, K_{\dot{H}}, K_{\ddot{H}}, K_{\int \dot{H}}] \tag{5}$$

The aircraft is supposed to track the predefined vertical rate command with requirements such as a rapid rise time, a minimum overshoot and a high steady accuracy. These requirements can be defined in the time domain as follows [20]

$$\text{Rise time: } f_{rt} = t_2|_{\dot{H}(t_2)=0.9\dot{H}_c} - t_2|_{\dot{H}(t_2)=0.1\dot{H}_c} \tag{6}$$

$$\text{Overshoot: } f_o = \max_{t>0} \left| \frac{\dot{H}(t)}{\dot{H}_c} \right| \tag{7}$$

$$\text{Steady accuracy: } f_{sa} = \max_{t>5} \left| \dot{H}(t) - \dot{H}_c \right| \tag{8}$$

where t is the simulation time and $\dot{H}_c$ is a step H-dot command.

In addition, two constraints (i.e., the angle of attack error and the stabilator command) are considered in the control system. The angle of attack error is computed by comparing the attack angle and the command α_c [20]

$$f_{aoa} = \int_{t>5} |\alpha(t) - \alpha_c| \tag{9}$$

The integration of stabilator command is introduced to avoid the overreaction. It can be calculated as [20]

$$f_{sc} = \int_{t>0} |\delta_s| \tag{10}$$

Thus, based on those five requirements, the cost function in the ACLS control parameter optimization

problem is designed using the weighted linear combination method as follows

$$f = \omega_1 f_{rt} + \omega_2 f_o + \omega_3 f_{sa} + \omega_4 f_{aoa} + \omega_5 f_{sc} \quad (11)$$

After converting the control parameter design problem to an optimization problem, the cost function can be optimized using the optimization algorithm. In this paper, the PIO algorithm is introduced to solve the optimization problem.

3 Pigeon-inspired optimization algorithm

The pigeon-inspired optimization algorithm is a new evolutionary algorithm inspired by the homing behavior of pigeons [21]. Pigeons can find their homes through homing tools including the magnetic field, the sun and landmarks. The magnetic field is used to shape the map and adjust the homing direction based on the altitude of the sun. Landmarks neighboring pigeons help them fly close to the destination. To mimic the natural phenomena, the PIO algorithm utilizes two operators to describe the flocking behavior of homing pigeons. In the PIO algorithm, the map and compass operator represents effects of the magnetic field and the sun, and the landmark operator describes the effects of landmarks.

Each pigeon in the flock represents a solution of the problem. The pigeon with the highest fitness value is selected as the potential solution of the problem. Given the population size N, the kth pigeon is defined by its position $X_k = [x_{k1}, x_{k2}, \ldots, x_{km}]$ and velocity $V_k = [v_{k1}, v_{k2}, \ldots, v_{km}]$, where m is the dimension of the solution.

In the map and compass operator, the new position and velocity of each pigeon are updated as follows [21]

$$V_k(t) = V_k(t-1) \cdot e^{-Ft} + rand \cdot (X_g - X_k(t-1)) \quad (12)$$

$$X_k(t) = X_k(t-1) + V_k(t) \quad (13)$$

where X_g denotes the best position in the flock, t is the iteration number, *rand* is a random number within [0, 1] and F is a factor which controls the rate of the velocity change.

In the landmark operator, half the pigeons are chosen to generate the center of the whole flock. Then pigeons move with a local gather strategy. The center can be calculated by [21]

$$C(t) = \frac{\sum_{N_p} X_k(t) \cdot fitness(X_k(t))}{\sum_{N_p} fitness(X_k(t))} \quad (14)$$

where N_p is a decreased number of the population size in the current iteration and $fitness(\cdot)$ represents the evaluation of the cost function. As a result of the landmark operator, all pigeons are driven to follow the center of the flock. Each pigeon updates its position using the following equation [21]

$$X_k(t) = X_k(t-1) + rand \cdot (C(t) - X_k(t-1)) \quad (15)$$

In fact, the update strategies of velocity and position have some similarities to the procedures in the PSO algorithm [27,28]. The PIO algorithm can be regarded as a combination of the standard PSO algorithm and a local gather strategy. However, as a population-based optimization tool, the PIO algorithm employs the experience of the whole flock instead of the experience of each individual, which is different from the PSO algorithm.

As the landmark operator in the basic PIO algorithm introduces the center of a decreased number of pigeons, pigeons would gather too quickly. When pigeons move to the center, two pigeons may be at the same position and update their positions synchronously. What's more, pigeons with worse fitness values are abandoned in the landmark operators of the basic PIO algorithm. The number of pigeons is decreased in the landmark operator, which could accelerate the convergence rate but lead to the lack of the diversity of population. In this paper, to keep the population size, the local gather strategy is implemented for all pigeons not only for the decreased number of pigeons.

In addition, the basic PIO algorithm chooses two operators using a threshold number of iteration. The map and compass operator is first selected and the landmark operator is used when the threshold is exceeded, which is not satisfied with the switching behavior of navigational states. Pigeons are switching between navigational states frequently when they overfly ground features that do or do not prompt positional reassessment [29]. There is no single navigational state when pigeons using homing tools. It means that pigeons have no fixed periods to choose the map and compass operator or the landmark operator. Thus, inspired by the uncertain navigational strategy of pigeons, a probability factor is introduced for the operator selection. The corresponding operator is selected based on the random number. If $rand < prob$, the map and compass

operator is selected to update positions on the basis of the current best one; otherwise, the landmark operator is used to gather pigeons around the center. In the MPIO algorithm, the new position and velocity of each pigeon are updated according to the probability factor as follows

$$V_k(t) = \begin{cases} V_k(t-1) \cdot e^{-Ft} + rand \cdot (X_g - X_k(t-1)) & \text{if } rand \le prob \\ rand \cdot (C(t) - X_k(t-1)) & \text{if } rand > prob \end{cases} \tag{16}$$

$$X_k(t) = X_k(t-1) + V_k(t) \tag{17}$$

Thus, the MPIO algorithm works as follows:

Step 1 Initialize the basic parameters of the algorithm, such as the population size N, the dimension m, the maximum number of iteration *Iter* and initial random set of pigeons.

Step 2 Evaluate all solutions by the cost function and select the pigeon with the highest fitness value as the current global best one.

Step 3 Select the operator based on the random number and the probability factor.

Step 4 Update the position and velocity of each pigeon according to the selected operator.

Step 5 Evaluate new solutions and update the global best one.

Step 6 Go to Step 3 for the next iteration if needed.

Given that $F = O(F)$ is the computational complexity of the cost function, the computational complexity of the map and compass operator is $O(Nm)$, and the computational complexity of the landmark operator is $O(Nm)$. Thus, the computational complexity of the MPIO is $O(Iter \cdot Nm)$. The modified procedure leads to no extra computation cost. Therefore, the MPIO can acquire the optimized solution within an acceptable period.

4 Simulation results and analysis

To measure the performance of our method, series of experiments are conducted. All experiments are performed using MATLAB R2012b on a PC with a Core II 2.4 GHz CPU and 3G of RAM.

4.1 Results on inner loop control parameter optimization

Firstly, the inner loop is optimized by fitting the frequency response curve with a desired frequency response curve. The frequency response curve in [20] is adopted in this paper. The number of sampling points is set to be 100 (i.e., $N_S = 100$). The trim values of the states are set as [20]: $V_0 = 69.96$ m/s, $\gamma_0 = -3.5$ deg and $\alpha_0 = 8.1$ deg. Parameters of the MPIO algorithm are set as: $N = 100$, $m = 3$, $F = 0.3$, $Iter = 50$ and $prob = 0.8$.

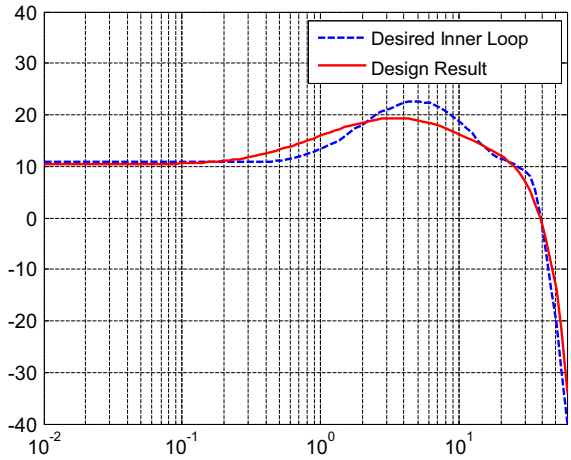

Fig. 4 Comparative frequency response of the inner loop

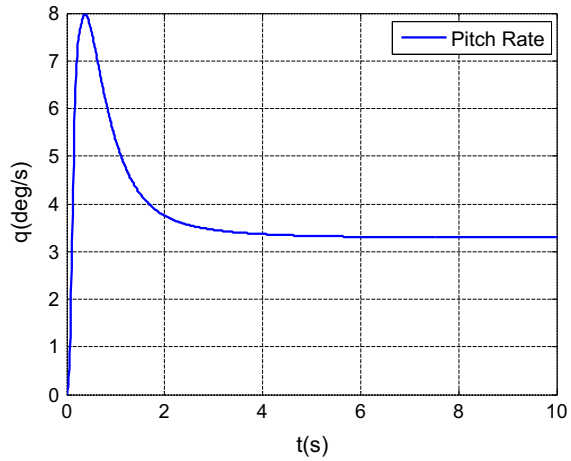

Fig. 5 Pitch rate response

The frequency response and the pitch rate response of the optimized inner loop are shown in Figs. 4 and 5, respectively. The frequency response curve in the low-frequency domain is similar to the desired curve. The rapid and steady response of pitch rate is consistent with expectation. As there are differences in the control structure, our optimized system cannot coincide with the desired curve between 0.3 rad/s and 20 rad/s.

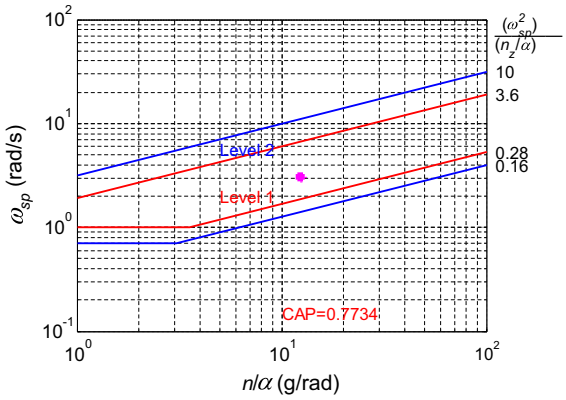

Fig. 6 CAP evaluation of the optimized inner loop

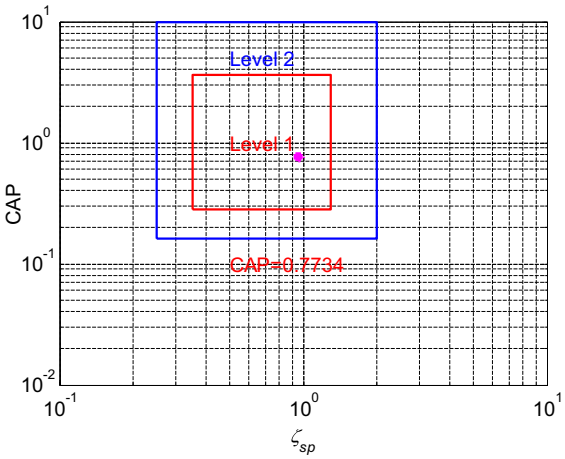

Fig. 7 Evaluation of the handing quality

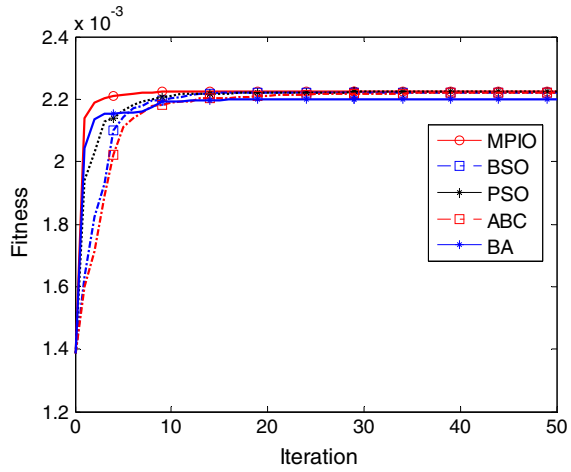

Fig. 8 Comparative evolutionary curves

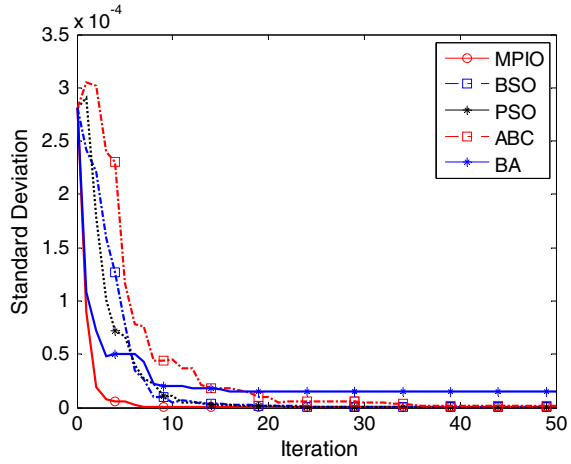

Fig. 9 Comparative standard deviation curves in 10 runs

To verify the performance of the optimized inner loop, the low-order equivalent system method is introduced to analyze the handling quality [20]. The control anticipation parameter (CAP) of the low-order equivalent system is evaluated. The CAP is defined as the ratio of initial pitch acceleration to steady-state normal acceleration in response to a step longitudinal control input. The CAP can indicate the problems associated with directly analyzing the short-period component of the high-order system responses with respect to the MIL-F-8785C short-period requirements [30]. In general, different level regions are defined on the basis of the pilot opinion data. If the CAP is within the Level 1 region, it reveals that the designed control system makes the aircraft be easily maneuvered. From evaluation results in Figs. 6 and 7, we can see that the CAP falls in the Level 1 region, which indicates that out optimized inner loop satisfies Level 1 requirement.

Furthermore, comparative experiments of various intelligent optimization algorithms are conducted. Four algorithms are introduced, such as BSO [20], PSO [31], ABC [32] and BA [33]. Initialization parts of these optimization methods are the same, which can avoid the effect of initialization. Parameters such as the population size and the maximum iteration number are also consistent. Comparative experimental results are shown in Figs. 8, 9 and 10. The MPIO algorithm has a fast convergence speed and the minimum standard deviation in multiple runs. Therefore, our proposed MPIO algorithm is superior to other algorithms.

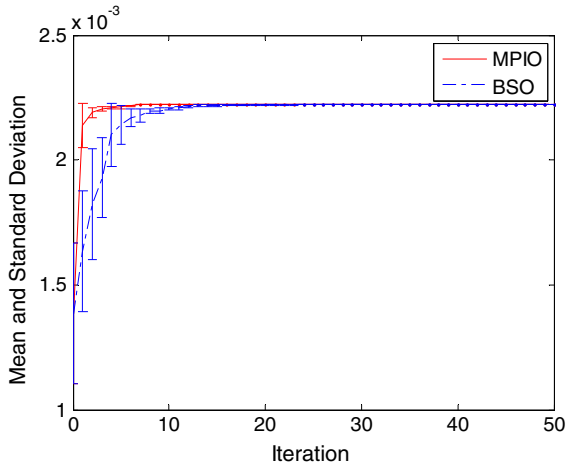

Fig. 10 Error bars of MPIO and BSO in 10 runs

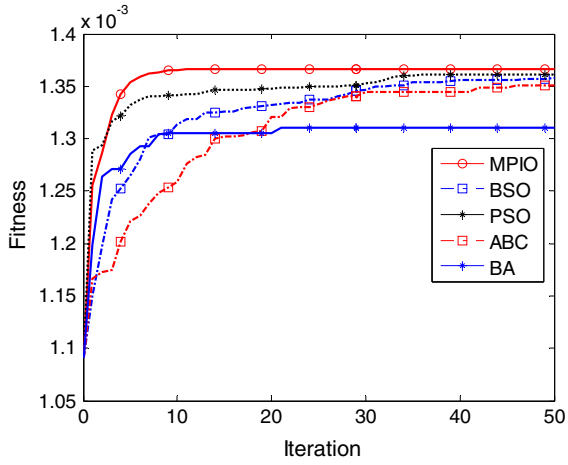

Fig. 11 Comparative evolutionary curves of the ACLS optimization

4.2 Results on ACLS control parameter optimization

Based on the optimized inner loop, control parameters in the APCS and the autopilot are determined in the same way. In the control structures shown in Figs. 2 and 3, eight parameters are optimized altogether. A step H-dot command is set to be 5 m/s, and the constant attack angle reference is set to be 0 deg [20]. The same weights in the weighted linear cost function are adopted. The dimension of the optimization problem is set to be $m = 8$. The other parameters are the same as those in the inner loop optimization.

Comparative evolutionary curves are shown in Fig. 11. Comparative experimental results of the MPIO and PIO are shown in Figs. 12 and 13. The MPIO algorithm has a fast convergence speed and better performance. The comparative results of vertical rate response in Fig. 13 indicate that our proposed method can achieve a more rapid rise time and less overshoot. Thus, the optimized control parameters are capable of ensuring the autopilot track the H-dot command quickly and precisely.

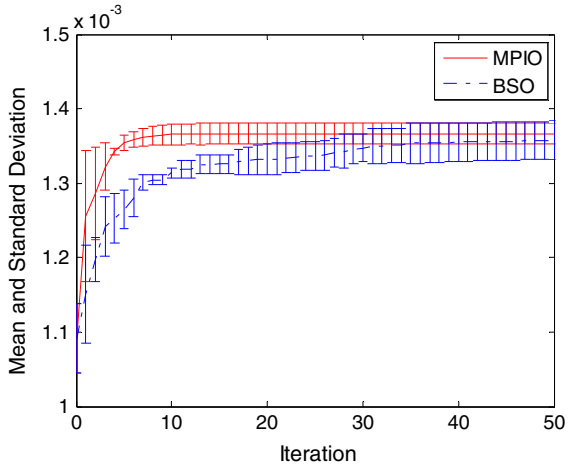

Fig. 12 Error bars of MPIO and BSO

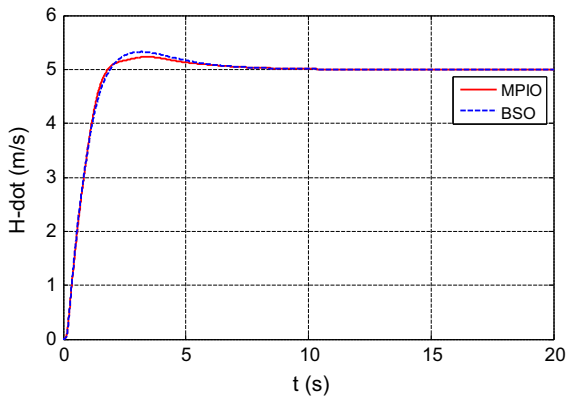

Fig. 13 Comparative results of vertical rate response

5 Conclusions and future work

This paper presented a novel control parameter design method for the ACLS. In general, a satisfied performance of landing on carriers in carious severe weather conditions can hardly be achieved by manual control. The empirical parameter adjustment is time-consuming

and full of challenge. The PIO algorithm is introduced to automatically optimize parameters in the control system. A modified version is proposed by introducing a probability factor for the operator selection and implementing the local gather strategy for all pigeons not only for the decreased number of pigeons. Experimental results demonstrate that our method is an effective tool to deal with the control parameter optimization problem. Comparative results indicate that our method is superior to other algorithms.

Our future work will focus on the design of closed-loop guidance law for the carrier landing system. Another aspect in which we would like to further improve our model is to design parameters in ACLS using multi-objective optimization methods.

Acknowledgments This work was partially supported by National Natural Science Foundation of China under grant #61425008, #61333004 and #61273054, National Key Basic Research Program of China (973 Project) under grant #2014CB046401, and Aeronautical Foundation of China under grant #2015ZA51013. The authors would like to thank the editors and reviewers for their critical review of this manuscript.

References

1. Martorella, P., Kelly, C., Nastasi, R.: Precision flight path control in carrier landing approach—a case for integrated system design. AIAA Aircraft Systems and Technology Conference, Dayton, Ohio, USA, AIAA-81-1710, pp. 1–10 (1981)
2. Urnes, J.M., Hess, R.K.: Development of the F/A-18A automatic carrier landing system. J. Guid Control Dyn **8**(3), 289–295 (1985)
3. Urnes, J.M., Hess, R.K., Moomaw, R.F., Huff, R.W.: Development of the navy H-dot automatic carrier landing system designed to give improved approach control in air turbulence. AIAA Guidance and Control Conference, New York, USA, AIAA-79-1772, pp. 491–501 (1979)
4. Craig, S.J., Ringland, R.F., Ashkenas, I.L.: An analysis of navy approach power compensator problems. J. Aircr. **9**(10), 737–743 (1972)
5. Zhu, Q., Wang, T., Zhang, W., Zhou, F.: Variable structure approach power compensation system design of an automatic carrier landing system. Control and Decision Conference, Guilin, China, pp. 5517–5521 (2009)
6. Urnes, J.M., Hess, R.K., Moomaw, R.F., Huff, R.W.: H-dot automatic carrier landing system for approach control in turbulence. J. Guid. Control Dyn. **4**(2), 177–183 (1981)
7. Prickett, A.L., Parkes, C.J.: Flight testing of the F/A-18E/F automatic carrier landing system. In: Proceedings of IEEE Aerospace Conference, Montana, USA vol. 5, pp. 2593–2612 (2001)
8. Steinberg, M.L.: Development and simulation of an F/A-18 fuzzy logic automatic carrier landing system. In: Proceedings of the Second IEEE International Conference on Fuzzy Systems, San Francisco, USA, vol. 2, pp. 797–802 (1993)
9. Subrahmanyam, M.B.: H-infinity design of F/A-18A automatic carrier landing system. J. Guid. Control Dyn. **17**(1), 187–191 (1994)
10. Crassidis, J.L., Mook, D.J.: Robust control design of an automatic carrier landing system. AIAA Astrodynamics Conference, Hilton Head Island, USA, AIAA-92-4619, pp. 1471–1481 (1992)
11. Steinberg, M.L., Page, A.B.: A comparison of neural, fuzzy, evolutionary, and adaptive approaches for carrier landing. AIAA Guidance, Navigation, and Control Conference and Exhibit, Montreal, Canada, AIAA-2001-4085, pp. 1–11 (2001)
12. Baker, W.L., Farrell, J.A.: Learning augmented flight control for high performance aircraft. AIAA Guidance, Navigation, and Control Conference, New Orleans, USA, AIAA-91-2836, pp. 347–358 (1991)
13. Steinberg, M.L., Page, A.B.: Nonlinear adaptive flight control with genetic algorithm design optimization. Int. J. Robust Nonlinear Control **9**(14), 1097–1115 (1999)
14. Lan, X., Wang, Y., Liu, L.: Dynamic decoupling tracking control for the polytopic LPV model of hypersonic vehicle. Sci. China Inf. Sci. **58**(9), 1–14 (2015)
15. Akay, B., Karaboga, D.: A modified artificial bee colony algorithm for real-parameter optimization. Inf. Sci. **192**, 120–142 (2012)
16. Qian, C., Yu, Y., Zhou, Z.: Variable solution structure can be helpful in evolutionary optimization. Sci. China Inf. Sci. **58**(11), 1–17 (2015)
17. Brest, J., Zumer, V., Maucec, M.S.: Self-adaptive differential evolution algorithm in constrained real-parameter optimization. IEEE Congress on Evolutionary Computation, Vancouver, Canada, pp. 215–222 (2006)
18. Duan, H., Wang, X.: Biologically adaptive robust mean shift algorithm with Cauchy predator–prey BBO and space variant resolution for unmanned helicopter formation. Sci. China Inf. Sci. **57**, 112202:1–112202:13 (2014)
19. Krishnakumar, K., Goldberg, D.E.: Control system optimization using genetic algorithms. J. Guid. Control Dyn. **15**(3), 735–740 (1992)
20. Li, J., Duan, H.: Simplified brain storm optimization approach to control parameter optimization in F/A-18 automatic carrier landing system. Aerosp. Sci. Technol. **42**, 187–195 (2015)
21. Duan, H., Qiao, P.: Pigeon-inspired optimization: a new swarm intelligence optimizer for air robot path planning. Int. J. Intell. Comput. Cybernet. **7**(1), 24–37 (2014)
22. Zhao, J., Zhou, R.: Pigeon-inspired optimization applied to constrained gliding trajectories. Nonlinear Dyn. **82**(4), 1781–1795 (2015)
23. Li, C., Duan, H.: Target detection approach for UAVs via improved pigeon-inspired optimization and edge potential function. Aerosp. Sci. Technol. **39**, 352–360 (2014)
24. Zhang, B., Duan, H.: Three-dimensional path planning for uninhabited combat aerial vehicle based on predator–prey pigeon-inspired optimization in dynamic environment. IEEE/ACM Trans. Comput. Biol. Bioinf. doi:10.1109/TCBB.2015.2443789 (in press, 2016)
25. Duan, H., Wang, X.: Echo state networks with orthogonal pigeon-inspired optimization for image restoration. IEEE

Trans. Neural Netw. Learn. Syst. in press, doi:10.1109/TNNLS.2015.2479117 (2016)
26. Yuan, Y.: A dynamic games approach to H∞ control design of DoS with application to longitudinal flight control. Sci. China Inf. Sci. **58**(9), 1–10 (2015)
27. Duan, H., Sun, C.: Pendulum-like oscillation controller for micro aerial vehicle with ducted fan based on LQR and PSO. Sci. China Technol. Sci. **56**(2), 423–429 (2013)
28. Zhao, Z., Wu, X., Lu, C., Glotin, H., Gao, J.: Optimizing widths with PSO for center selection of Gaussian radial basis function networks. Sci. China Inf. Sci. **57**(5), 1–17 (2014)
29. Guilford, T., Roberts, S., Biro, D., Rezek, I.: Positional entropy during pigeon homing II: navigational interpretation of Bayesian latent state models. J. Theor. Biol. **227**(1), 25–38 (2004)
30. Bischoff, D.: The definition of short-period flying qualities characteristics via equivalent systems. J. Aircr. **20**(6), 494–499 (1983)
31. Pires, E.J.S., Machado, J.A.T., de Moura Oliveira, P.B., et al.: Particle swarm optimization with fractional-order velocity. Nonlinear Dyn. **61**(1–2), 295–301 (2010)
32. Li, X., Yin, M.: Parameter estimation for chaotic systems by hybrid differential evolution algorithm and artificial bee colony algorithm. Nonlinear Dyn. **77**(1–2), 61–71 (2014)
33. Yang, X.S.: A New Metaheuristic Bat-Inspired Algorithm. Nature Inspired Cooperative Strategies for Optimization (NICSO 2010). Springer, Berlin (2010)